# Modelling of transient liquid phase bonding

Y. Zhou, W. F. Gale, and T. H. North

Modelling of transient liquid phase (TLP) bonding is reviewed. The outputs produced during analytical and numerical modelling are discussed in detail and compared with actual experimental results produced when joining simple binary alloy systems. The effects of increased diffusivity at base material grain boundaries, of grain boundary motion, and of grain boundary grooving, on isothermal solidification during TLP bonding are described. There is a critical need for detailed research in which modelling output is closely related to direct microstructural observations during bonding of complex alloy systems.

IMR/280


Dr Zhou is Research and Development Engineer, Fuel Materials Branch, AECL Research, Chalk River Laboratories, Chalk River, ON, Canada. Dr Gale is Assistant Professor, Materials Research and Education Center, Auburn University, Auburn, AL, USA. Dr North is WIC/NSERC Professor, Department of Metallurgy and Materials Science, University of Toronto, Toronto, ON, Canada.

## Introduction

Diffusion controlled growth or dissolution of an unstable phase is important in a wide range of metallurgical situations,[1–3] such as:

(i) in solid–gas (vapour) systems when an intermediate aluminide phase grows during aluminisation of nickel base alloy materials[4]

(ii) in solid–solid systems when a second phase grows and subsequently dissolves during solution heat treatment,[5] or when an intermediate layer grows in a thermal barrier coating[6]

(iii) in solid–liquid systems when the liquid phase grows and/or shrinks during liquid phase sintering[7] or during transient liquid phase (TLP) bonding.[8]

During TLP bonding, a thin layer of liquid forms at the joint interface, wets the contacting substrates, and then solidifies isothermally.[8,9] Liquid film formation during TLP bonding depends on the formation of a low melting point eutectic or peritectic at the joint interface. An interlayer (filler metal) is clamped between the contacting metal surfaces and the entire assembly is heated to the bonding temperature. At the bonding temperature, the interlayer forms a liquid, either directly or by reaction with the base metal. The resulting liquid film resolidifies isothermally when the joint is held at the bonding temperature. Following isothermal solidification, the joint is homogenised either at the bonding temperature or at some lower temperature. All stages of TLP bonding (interlayer and base metal melting, isothermal solidification and joint homogenisation) depend on solute diffusion from the joint centreline region into the base material.

In certain situations, liquid formation can occur without the introduction of an interlayer at the bondline. For example, solute diffusion during heating promotes formation of a low melting point eutectic in Zircaloy 2–AISI 304 stainless steel joints.[10] However, in this case, the liquid film width increases continuously at the bonding temperature. Since this is quite a different situation from that assumed during TLP bonding (where the liquid width increases to a maximum value before isothermal solidification) this joining process is generally termed eutectic bonding. As would be expected, the success of eutectic bonding depends on being able to produce a uniform temperature distribution across the whole joint and on careful control of bonding temperature and holding time.

Transient liquid phase bonding has been employed in a range of applications, since it produces joints that have microstructural and hence mechanical properties similar to those of the base material. Transient liquid phase bonding has the following advantages.

1. Joint formation depends on an isothermal, relatively low temperature bonding mechanism.
2. No interface remains after the TLP bonding operation.
3. Since the joining technique depends on capillary filling, the joint preparation before TLP bonding is relatively simple. Also, using the wide gap TLP bonding technique permits repair of defects up to 100 μm wide.[11,12]
4. In contrast to diffusion bonding,[13,14] the joining process is highly tolerant to the presence of a faying surface oxide layer. For this reason, and because of the absence of thermal stresses, TLP bonding is ideal when joining intermetallic base materials which have stable oxide surface films, are highly sensitive to microstructural changes, and have poor low temperature ductility.[15–18]
5. The bonding process is ideal when joining base materials which are inherently susceptible to hot cracking or post-weld heat treatment cracking problems.[19]
6. The bonding process is ideally suited for the fabrication of large and complex shaped components.

Transient liquid phase bonding has been used when joining nickel base and iron base superalloy materials,[9,12,20–40] when joining titanium alloys,[41–44] when joining stainless steel,[45] when joining aluminium,[46] when joining aluminium base and titanium base metal matrix composites,[47–54] during dissimilar joining of copper to austenitic stainless steel,[55] and when joining microcircuitry components.[56,57] Non-metals have also been joined using TLP bonding; for example, silicon nitride has been bonded at 1550°C using an oxynitride glass.[58] In this case, the key requirement is that the glass composition must be selected so that thermal expansion mismatch is minimised.

### Rationale for review

Although TLP bonding has been widely applied, the underlying basis for its use rests on empirical testing. Much published research on final joint quality emphasises the results of engineering assessments, i.e. evaluations of high temperature tensile strength, creep rupture strength, thermal shock resistance, corrosion resistance, fatigue properties, and so on. Considerable work is still required to provide a quantitative prediction of the optimum bonding conditions (interlayer composition, bonding temperature, holding time) during TLP bonding. However, much research has been carried out on modelling of diffusion controlled growth or dissolution of an unstable phase (as is encountered during TLP bonding) using analytical and finite element modelling techniques. In addition, a number of microstructural investigations (of varying detail) of TLP bonding have been completed.[59–64] With this in mind, the present review describes the status of research in process modelling of TLP bonding. The advantages and disadvantages of analytical and numerical modelling are discussed, based on a comparison of calculated output with the experimental results produced when examining simple binary alloy systems. Finally, the extent to which modelling output and microstructural observations can be correlated in complex alloy joints is reviewed. Since much research has been published on TLP bonding of nickel base superalloys, the results produced in this particular area are reviewed as an example of the application of modelling when joining complex alloy systems. The future needs in TLP bonding research are associated with the development of a much clearer relationship between modelling output and direct microstructural observations.

## Basis of process

### Stages in TLP bonding

Duvall *et al.*[9] examined TLP bonding of Ni–Cr–Co base superalloy material using Ni–B filler metal and suggested that the TLP bonding process comprised three different stages, namely, base metal dissolution, isothermal solidification of the liquid phase, and joint homogenisation. However, Tuah-Poku *et al.*[8] investigated TLP bonding of silver using pure copper filler metal and suggested that filler metal melting and widening of the liquid zone at the bonding temperature were separate stages. There is consequently some dispute concerning the detailed characteristics of the base metal dissolution stage.

MacDonald and Eagar[65] pointed out that a further stage should be included in TLP bonding in order to account for solute diffusion during the heating cycle to the bonding temperature. This assertion was based on an analysis of the experimental results published by Niemann and Garret[47] when they joined Al–B composite base material using thin copper foils. When the heating rate between room temperature and the eutectic temperature is very slow, insufficient liquid forms at the resulting bonding temperature (owing to diffusion of copper from the copper filler metal into the base material during the heating stage), and very poor joint mechanical properties are produced. It is worth emphasising that the heating rate between the eutectic temperature and the bonding temperature also has an important effect on the process kinetics which occur during TLP bonding. Solute diffusion in the temperature range from the filler metal melting point $T_M$ to the bonding temperature $T_B$ may allow solidification to occur before the selected bonding temperature is reached. This particular situation was modelled by Nakagawa *et al.*[66] during TLP bonding of Nickel 200 base metal using Ni–19 at.-%P filler metal. Solidification occurred when the heating rate between $T_M$ and $T_B$ was very slow ($\sim 1$ K s$^{-1}$) and when a thin (5 μm) filler metal was used. In addition, the likelihood of solidification at temperatures between $T_M$ and $T_B$ increased markedly when the filler metal contained a high diffusivity melting point depressant such as boron. It is worth noting that the heating rate from the eutectic temperature to the bonding temperature can be very slow unless inductive heating is employed during TLP bonding. For example, Zhou[67] obtained a heating rate of 2·5 K s$^{-1}$ between the eutectic temperature (850°C) and the bonding temperature (1150°C) when joining 10 mm long × 10 mm dia. cylindrical Nickel 200 test samples using Ni–19 at.-%P filler metal in a vertical radiation furnace.

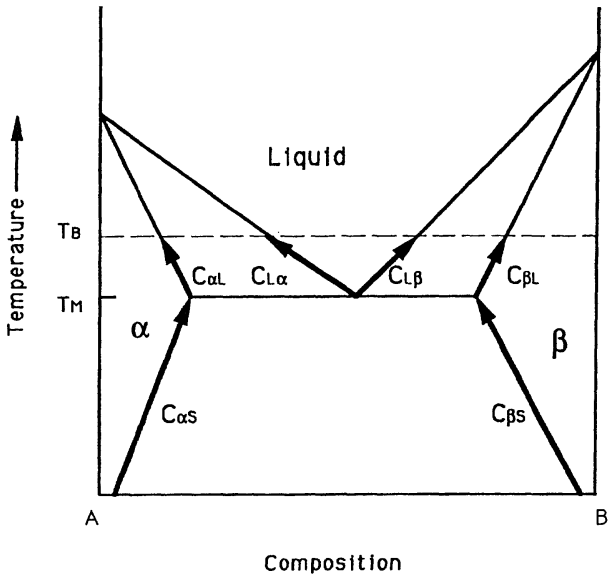


**1 Hypothetical binary phase diagram with eutectic point**

Based on the above commentary, the different stages during TLP bonding require further classification. With this in mind, an overall classification of the different stages in TLP bonding is presented below. It is convenient to describe this classification of TLP bonding using the binary eutectic equilibrium phase diagram and the time–temperature relationship shown in Figs. 1 and 2. It is worth noting that this classification equally applies when a eutectic alloy filler metal is employed (*see* Figs. 1 and 3*a*) and when a single element filler metal is used during TLP bonding (*see* Figs. 1 and 3*b*).

### Stage I

This is the heating stage, where the component is heated from room temperature to the filler metal

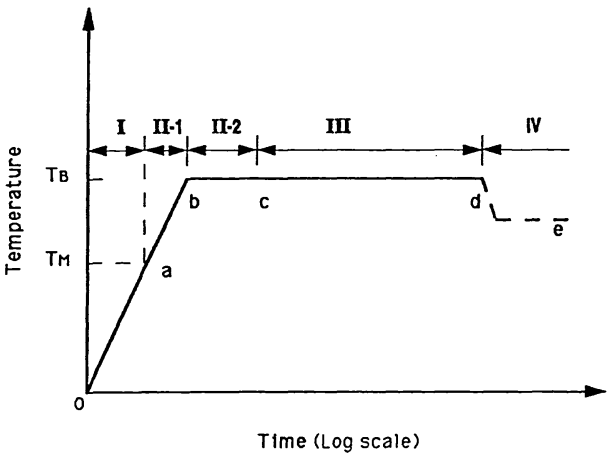


**2 Schematic showing different stages during heating cycle of TLP bonding, where $T_B$ is bonding temperature and $T_M$ is melting point of filler metal**

melting temperature (from point 0 to point a in Fig. 2). During heating, interdiffusion occurs between the filler metal and base material so that the solute concentration $C_{\alpha S}$ at the base material/filler metal interface changes with temperature following the solvus line in the binary phase diagram (*see* Fig. 1). Niemann and Garret[47] pointed out that the heating stage is particularly important when the filler metal is very thin (since all the filler metal can be consumed during heating to the bonding temperature). In this connection, Li *et al.*[54] examined TLP bonding of alumina bearing metal matrix composite material using thin copper foils and found that the minimum interlayer thickness for satisfactory joint formation increased from 0·6 to 2 μm when the heating rate decreased from 5 to 1 K $s^{-1}$.

## Stage II

This is the dissolution stage (from point a to point b and then to point c in Fig. 2), when the base metal dissolves into the liquid and hence the width of the liquid zone increases. This stage can be subdivided as follows.

### Stage II-1

In this stage, the temperature increases from the melting point to the bonding temperature (from point a to point b in Fig. 2) and the solute concentrations, $C_{L\alpha}$ and $C_{\alpha L}$, and $C_{L\beta}$ and $C_{\beta L}$ at the solid/liquid interfaces are changing with temperature following the solidus and liquidus lines in the binary phase diagram.

### Stage II-2

This is when isothermal dissolution occurs at the bonding temperature (from point b to point c in Fig. 2). When a single element interlayer *B* is used in the binary eutectic alloy system, three metallurgical phases (α, β, and liquid) are present at the beginning of the dissolution stage. Stages II-1 and II-2a (*see* Fig. 3*b*) proceed and the β-phase disappears during stage II-2b. At the end of stage II, the liquid zone has reached its maximum width.

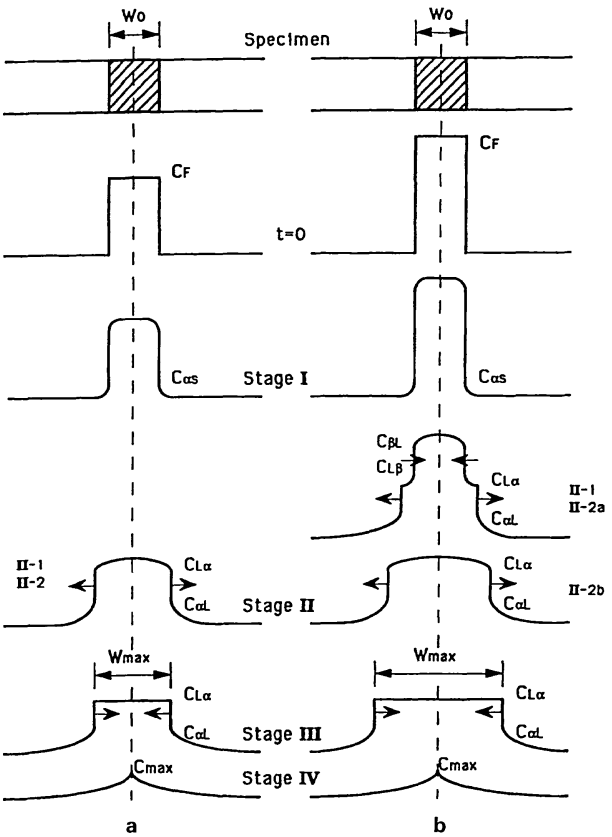


**3 Schematic showing concentration profiles during TLP bonding using *a* eutectic filler metal and *b* single element filler metal**

Again, it is worth noting that isothermal dissolution of the base metal might not occur at the bonding temperature if the heating rate between $T_M$ and $T_B$ is very slow and a thin eutectic composition filler metal containing a high diffusivity melting point depressant is used.[66]

## Stage III

This is the isothermal solidification stage, where the liquid zone solidifies as a result of solute diffusion into the base metal at the bonding temperature (from point c to point d in Fig. 2). The solute concentrations at the solid/liquid interface $C_{L\alpha}$ and $C_{\alpha L}$ are unchanged during this stage and the width of the liquid zone decreases continuously until the joint completely solidifies. The solute distribution in the liquid is uniform during almost all of the isothermal solidification stage.[66,68]

The isothermal solidification stage is generally considered to be the most important since the completion time required for the entire TLP bonding process is largely determined by the time required for completion of isothermal solidification (*see*, for example, Refs. 8, 69). This readily explains why much research has been carried out on this particular aspect of the bonding process.

## Stage IV

This is the homogenisation stage where solid state solute redistribution occurs (from point d to point e

in Fig. 2). The homogenisation temperature need not be that used during stages II and III and this operation is generally terminated when the maximum solute concentration at the joint centreline reaches some preselected value.

The two crucial factors in the TLP bonding process are that: the completed joint has a chemical composition located in the single phase region of the binary equilibrium phase diagram (Fig. 1); and the joining process approaches this end point through solute diffusion. Figure 3 confirms that use of a single element filler metal will markedly increase the maximum liquid width and hence the time required for joint completion during TLP bonding (compared with the situation when an equivalent thickness, eutectic composition filler metal is employed). However, it is important to emphasise that TLP bonding is a continuous process and Figs. 1–3 are only presented as a basis for understanding the physical phenomena that occur during the joining operation.

## Process modelling

Much modelling research to date has involved the use of analytical methods.[8,12,21,70,71] However, the analytical approach treats the joining process as a number of discrete steps and this is not what actually occurs during TLP bonding. For example, the completion time required for solute homogenisation will depend on the solute distribution immediately following completion of the isothermal solidification stage.[72] In addition, the analytical calculations for each stage of the joining process depend on the error function solution and parabolic law assumptions and these may be considered only as approximate solutions. In contrast, numerical modelling has the key advantage that it can treat base metal dissolution, isothermal solidification, and solute homogenisation as interdependent sequential processes. Furthermore, numerical modelling can be readily applied to two- or three-dimensional joining situations, or when the fabricated components have complicated shapes.

Local equilibrium at the migrating interface is generally assumed when modelling two phase diffusion controlled problems. However, this is an approximation, since local equilibrium is generally not attained at the solid/liquid interface.[73] Also, it is generally assumed that the formation of the liquid phase assures complete wetting of the base metal and production of a sound joint, and this may not necessarily be the case during TLP bonding.

### Basic solutions for diffusion equations

Analytical modelling of TLP bonding depends on classical solutions for Fick's diffusion equations.[74] For the sake of brevity, the present discussion will be limited to two cases only.

The first case occurs when the surface of a semi-infinite specimen with an initial solute concentration $C_M$ is maintained at composition $C_0$ for all $t>0$ values, i.e.

$$C(y,0)=C_M \quad (1)$$

$$C(0,t)=C_0 \quad (2)$$

where $t$ is time and $y$ the distance from the surface, and the solute concentration in the specimen is

$$C(y,t)=C_0+(C_M-C_0)\,\mathrm{erf}\left(\frac{y}{(4Dt)^{1/2}}\right) \quad (3)$$

where $D$ is the solute diffusion coefficient. The rate at which the diffusing species enters the specimen is given by the relation

$$\left(D\frac{\partial C}{\partial y}\right)_{y=0}=\frac{D(C_M-C_0)}{(\pi Dt)^{1/2}} \quad (4)$$

The total amount $M_t$ of diffusing substance which has entered the medium at time $t$ is found by integrating the above equation with respect to $t$

$$M_t=2(C_0-C_M)\left(\frac{Dt}{\pi}\right)^{1/2} \quad (5)$$

The second case is when the initial thickness ($2h$) of the source of the diffusing species ($C_0$) is of the order of the diffusion distance $(Dt)^{1/2}$, i.e.

$$C(y,0)=C_0 \qquad h\geqslant y\geqslant 0 \quad (6)$$

$$C(y,0)=C_M \qquad y>h \quad (7)$$

where $C_M$ is the initial concentration of diffusant in the specimen. The solute concentration is given by the relation

$$C(y,t)=C_M+\frac{1}{2}(C_0-C_M)\times\left\{\mathrm{erf}\left[\frac{y+h}{(4Dt)^{1/2}}\right]-\mathrm{erf}\left[\frac{y-h}{(4Dt)^{1/2}}\right]\right\} \quad (8)$$

### Analytical solutions for TLP bonding

As pointed out above, analytical solutions have been derived for each individual stage in TLP bonding. It is tacitly assumed that the output of any stage does not affect the operating conditions that apply in subsequent stages of the TLP bonding process.

#### Heating stage

Equation (5) was used by Niemann and Garret[47] to calculate the loss of the copper from an electroplated copper layer during the heating cycle from room temperature to the bonding temperature (when joining Al–B composite material). They developed the relation

$$x\rho_c=1{\cdot}1284\rho_a(C_{\alpha S}-C_M)(D_S t)^{1/2} \quad (9)$$

where $x$ is the thickness of copper coating lost through diffusion, $\rho_c$ the density of copper, $D_S$ the diffusion coefficient of copper in aluminium, $t$ time, $C_{\alpha S}$ the solubility of copper in aluminium, $\rho_a$ the density of the alloy, and $C_M$ the initial copper concentration in the aluminium substrate. Niemann and Garret assumed constant $C_{\alpha S}$ and $D$ values in their calculations. However, both the diffusion coefficient and solid solubility limit increase with temperature. With this in mind, MacDonald and Eagar[65] suggested this problem could be overcome through the use of the effective diffusion coefficient proposed by Shewmon.[75] It is worth pointing out that this diffusion problem is easily solved using numerical techniques.[54]

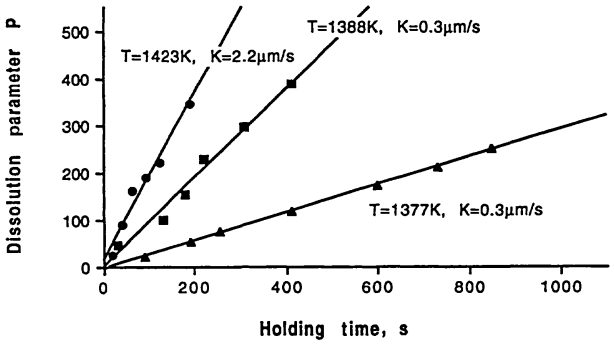


**4 Relation between the dissolution parameter *P* and holding time at various holding temperatures (during TLP bonding of nickel base superalloy material MBF-007 using and MBF-80 filler metal) (after Ref. 31)**

### Dissolution stage

No analytical solution is available for stage II-1 of TLP bonding (base metal dissolution during the heating cycle from the eutectic temperature to the bonding temperature) since the solute concentrations $C_{L\alpha}$ and $C_{\alpha L}$ at the interface vary with temperature. In this connection, only limited work has been carried out to determine the process kinetics during stage II-2 of the TLP bonding process (base metal dissolution at the bonding temperature).

Nakao *et al.*[31] examined isothermal dissolution during TLP bonding (stage II-2 in Fig. 2) and, based on the Nernst–Brunner theory (*see* Ref. 66), developed a dissolution parameter $P$

$$P = Kt = h \ln\left[\frac{W_0(W_t + ph)}{ph(W_0 - W_t)}\right] \quad . \; . \; . \; . \; . \; . \; . \quad (10)$$

where $W_t$ is the width of base metal dissolved at time $t$, $W_0$ the equilibrium (saturated) dissolution width, $\rho$ the ratio of the densities of the liquid and solid phases, $h$ half of the initial liquid width, and $K$ a constant. During TLP bonding of nickel base superalloy base material using Ni–15·5 wt-%Cr filler metal, this dissolution parameter was related linearly to holding time (*see* Fig. 4). Nakao *et al.*[31] therefore concluded that the Nernst–Brunner theory could be used to explain dissolution during TLP bonding. However, Nakagawa *et al.*[66] pointed out that the key assumptions of a thin boundary layer and a large bulk liquid region in the Nernst–Brunner theory did not apply during TLP bonding, and solute diffusion into the base metal was neglected in the calculations made by Nakao *et al.* It is worth noting that the width of the liquid layer was held constant during the TLP bonding experiments carried out by Nakao *et al.* When, however, silver base metal was TLP bonded using copper filler metal, the liquid width formed at the bonding temperature was not held constant, and a non-linear relation was observed between the dissolution parameter and holding time.[8,66]

Lesoult[70] applied a square root law solution to estimate the time required for interlayer melting when a pure metal interlayer was used in a binary eutectic alloy system. However, MacDonald and Eagar[65] have pointed out that Lesoult's assumption that the final width of the liquid zone equals the interlayer width (when melting of the interlayer is completed) is doubtful, since base metal dissolution occurs when the interlayer melts. In this connection, Liu *et al.*[76] developed a model that accounts for base metal melting during liquid formation. They used a general error function solution to describe the solute distribution in the liquid zone when modelling stage II-2a (the dissolution stage when three metallurgical phases exist) and assumed that there was no solute diffusion into the base metal. These assumptions are questionable. The error function solution is really only applicable for infinite or semi-infinite media, and the liquid zone is very thin in comparison with the solute diffusion rate in the liquid during TLP bonding. Furthermore, solute diffusion into the base metal can affect the process kinetics during stage II of TLP bonding.[8]

In summary, analytical methods are difficult to apply during modelling of the dissolution stage during TLP bonding. It is shown in the section 'Comparison of numerical and analytical output', below, that numerical methods are more efffective when solving this particular problem.

### Isothermal solidification

Solute distribution in the liquid can be considered uniform during the isothermal solidification stage of TLP bonding,[66,67] and therefore, solute diffusion in the liquid can be ignored. In addition, the base metal can be assumed to be semi-infinite because solute diffusion in the solid is relatively slow. The isothermal solidification stage during TLP bonding can be analytically modelled as a single phase diffusion controlled moving interface problem (*see* Fig. 5).

Lynch *et al.*[77] first linked interface movement with the mass balance at the liquid/solid interface but failed to provide an analytical solution for this problem. Tuah-Poku *et al.*[8] proposed a method for estimating the completion time required to the isothermal solidification stage of TLP bonding. In their treatment, the problem was simplified to a half semi-infinite base metal with a surface on which the solute concentration was maintained at $C_{\alpha L}$. Consequently, an error function solution can be employed to describe the solute distribution in the base metal

$$C(y, t) = C_{\alpha L} + C_{\alpha L} \operatorname{erf}\left[\frac{y}{(4D_S)^{1/2}}\right] \quad . \; . \; . \; . \quad (11)$$

where $C_{\alpha L}$ is the solute concentration in solid at the interface. The total solute amount $M_t$ that has entered the base metal at time $t$ can be calculated from the relation

$$M_t = 2C_{\alpha L}\left(\frac{D_S t}{\pi}\right)^{1/2} \quad . \; . \; . \; . \; . \; . \; . \; . \; . \; . \quad (12)$$

If the amount of solute diffused into the base metal during the heating and dissolution stages is ignored, the total amount of solute diffused into the base metal equals the original solute content of the filler metal, i.e.

$$C_F W_0 = 4C_{\alpha L}\left(\frac{D_S t}{\pi}\right)^{1/2} \quad . \; . \; . \; . \; . \; . \; . \; . \; . \; . \quad (13)$$

where $C_F$ is the solute content in the filler metal and

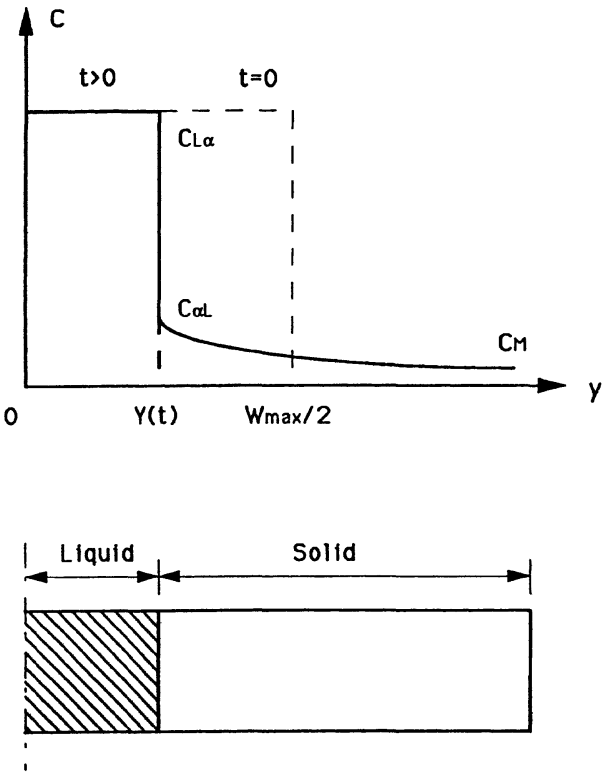


**5 Concentration profile along specimen length during isothermal solidification stage**

$W_0$ the initial width of the filler metal. The completion time for isothermal solidification can therefore be calculated using the relation

$$t_S = \frac{\pi}{16D_S}\left(\frac{C_F W_0}{C_{\alpha L}}\right)^2 \quad . \; . \; . \; . \; . \; . \; . \; . \; . \; . \; (14)$$

Similar treatments of this problem have been reported by Ikawa *et al.*,[22] Nakao *et al.*,[31] and Onzawa *et al.*[49]

A more rigorous treatment of the problem was presented by Lesoult.[70] His derivation is almost identical with that described by Danckwerts,[78] when he derived a general solution for unsteady state linear heat conduction or diffusion. A general error function solution is assumed in the solid phase

$$C_S(y, t) = A_1 + A_2 \operatorname{erf}\left[\frac{y}{2(D_S t)^{1/2}}\right] \quad . \; . \; . \; . \; (15)$$

where $A_1$ and $A_2$ are constants determined by the specific boundary conditions. When $y \to \infty$

$$C_S(\infty, t) = A_1 + A_2 = C_M \quad . \; . \; . \; . \; . \; . \; . \; . \; (16)$$

and at the moving interface

$$C_S(Y, t) = A_1 + A_2 \operatorname{erf}\left[\frac{Y}{2(D_S t)^{1/2}}\right] = C_{\alpha L} \quad . \; . \; (17)$$

Since equation (17) has to be satisfied for all values of $t$, $Y$ must be proportional to $t^{1/2}$, i.e.

$$Y = K(4D_S t)^{1/2} \quad . \; . \; . \; . \; . \; . \; . \; . \; . \; . \; . \; . \; (18)$$

where $K$ is a constant. The mass balance at the interface produces the relation

$$(C_{L\alpha} - C_{\alpha L})\frac{dY(t)}{dt} = D_S\left(\frac{\partial C_S(y, t)}{\partial y}\right)_{y=Y(t)} \quad . \; . \; (19)$$

Solving equations (15) and (19) leads to

$$\frac{K(1 + \operatorname{erf} K)\pi^{1/2}}{\exp(-K^2)} = \frac{C_{\alpha L} - C_M}{C_{L\alpha} - C_{\alpha L}} \quad . \; . \; . \; . \; . \; (20)$$

Similar solutions were derived by Sakamoto *et al.*,[79] and Ramirez and Liu.[80] It is worth noting that in the derivations of Lesoult[70] and Liu *et al.*,[76] the term $\exp(-K^2)$ is higher than the fraction indicated in equation (20). Also, Le Blanc and Mevrel[36] used an identical derivation procedure to obtain a formulation which accounts for boron consumption as a result of boride formation during TLP bonding of nickel base superalloy base material.

The completion time for isothermal solidification during TLP bonding can be calculated using the relation

$$t_S = \frac{W_{max}^2}{16K^2 D_S} \quad . \; . \; . \; . \; . \; . \; . \; . \; . \; . \; . \; . \; (21)$$

where $W_{max}$ is the maximum liquid width calculated using the mass balance method.[8]

Derivation of equation (14) depends on the assumption that the solute distribution is given by equation (11) and this is only exact for a stationary interface. Since the liquid/solid interface migrates during TLP bonding, it is important to determine the conditions when this assumption can be applied. Solving equations (15)–(17), we obtain

$$C_S(y, t) = C_M - \frac{C_M - C_{\alpha L}}{1 - \operatorname{erf}(K)} + \frac{C_M - C_{\alpha L}}{1 - \operatorname{erf}(K)} \times \operatorname{erf}\left[\frac{y}{2(D_S t)^{1/2}}\right] \quad . \; . \; . \; . \; . \; . \; (22)$$

$K$ is the factor related to the solute distribution in equation (20) and therefore when $K \to 0$ and $\operatorname{erf}(K) \to 1$, equation (22) becomes

$$C_S(y, t) = C_{\alpha L} + (C_M - C_{\alpha L}) \operatorname{erf}\left[\frac{y}{2(D_S t)^{1/2}}\right] \quad (23)$$

This is identical to equations (3) and (11). It follows that the solute distribution in the solid can be calculated using equation (11) when $K$ is very small.

### Homogenisation stage

Equation (8) was used by Ikawa *et al.*[22] to model the solute distribution during homogenisation of TLP bonded nickel base superalloy material. In their formulation, $h$ was half the maximum liquid width at the end of the base metal dissolution period and $C_0$ equalled $C_{L\alpha}$. The solute concentration attained its maximum value at the centreline of the specimen ($x = 0$) when,

$$C_{max} = C(0, t) = C_M + (C_0 - C_M) \times \operatorname{erf}\left[\frac{h}{4(D_S t)^{1/2}}\right] \quad . \; . \; . \; . \; . \; . \; . \; (24)$$

When examining the aluminium redistribution during

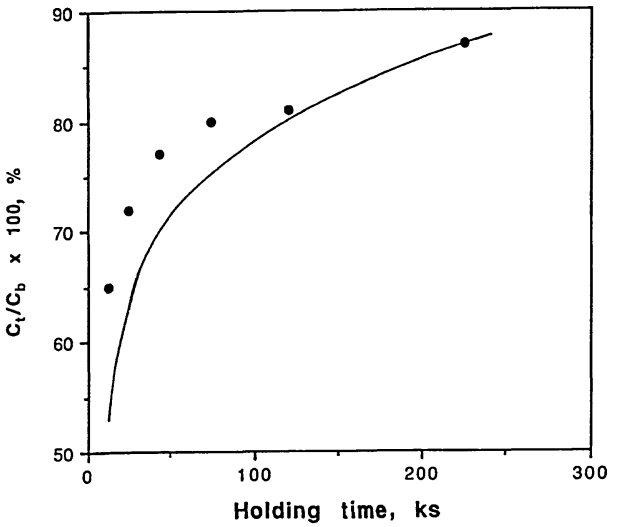


● experimental test results
—— calculated results.

**6 Calculated and experimentally measured aluminium concentrations at the joint centreline during homogenisation of TLP bonded nickel base superalloy material using MBF-80 filler metal at 1453 K (after Ref. 12): $C_t$ is concentration of aluminium at time $t$; $C_b$ is aluminium concentration in base metal**

homogenisation of nickel base superalloy material, Nakao *et al.*[31] observed close agreement between the results calculated using equation (24) and the experimental values (for much of the homogenisation period). However, there was a distinct difference between the analytical calculations and the experimental values during the early stages of the homogenisation treatment (*see* Fig. 6). Nakao *et al.*[12] suggested that this difference was due to a critical assumption in the analytical results (that the aluminium concentration in the joint centreline was uniform at the beginning of the homogenisation period).

Zhou[67] also used equation (24) to model the homogenisation stage during TLP bonding. In that study, $h$ was half the filler metal thickness ($W_0/2$), and $C_0$ the initial solute concentration in the filler metal $C_F$. This particular approach has the advantage that the maximum liquid width need not be calculated using equation (24).

## Numerical simulation of TLP bonding

Nakagawa *et al.*[66] modelled dissolution behaviour during TLP bonding of Nickel 200 base metal using Ni–P and Ni–Cr–P filler metals. This research confirmed the critical effect that both the filler metal thickness, and the heating rate between the filler metal melting temperature and the bonding temperature had on the base metal dissolution process. An explicit finite difference method was employed to calculate solute diffusion in liquid and solid phases and a stepwise 'mechanical' mass balance method was used to determine solid/liquid interface movement. However, the approach of Nakagawa *et al.* had inherent problems, since the exact location of the solid/liquid interface could be determined using the stepwise mass balance technique, and extremely long

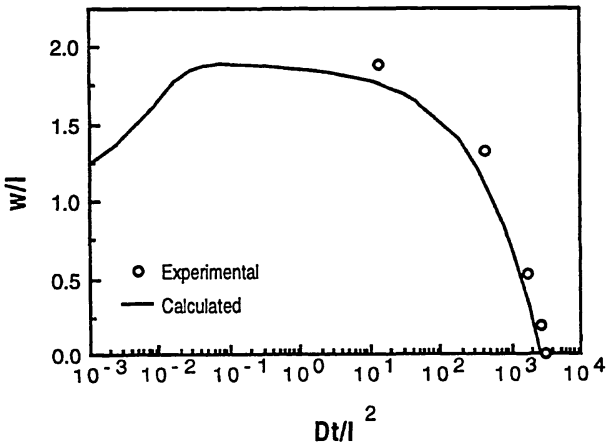


**7 Comparison of calculated and experimental results during TLP bonding of single crystal nickel (after Ref. 67)**

calculation times were required when the whole TLP bonding process was modelled.

These problems were overcome by developing a fully implicit finite difference model that simulated the TLP bonding process in a continuous manner.[81] Figure 7 compares the calculated and experimental test results during TLP bonding of single crystal nickel. The results are in excellent agreement and a short computation time is required. This numerical model output can be used to:

(i) predict the completion times required for dissolution, isothermal solidification, and homogenisation
(ii) predict the solute concentration distribution both in the solid phase and in the liquid phase throughout TLP bonding (*see* Figs. 8–10); these results cannot be calculated using analytical methods[80]
(iii) select the optimum filler metal (chemistry, thickness) and bonding temperature which will ensure that the TLP bonding operation is completed in a reasonable time frame
(iv) examine diffusion controlled, two phase moving interface problems other than TLP bonding; for example, the fully implicit finite difference model has been applied to the solution treatment of thin multilayer $\alpha$ and $\beta$ brass diffusion couples.[81–83]

Figure 11 shows the influence of changes in the equilibrium solute content in solid at the bonding temperature $C_{\alpha L}$ on the completion times required for base metal dissolution, isothermal solidification, and homogenisation. $C_{\alpha L}$ can be varied by altering the solute content in the filler metal or by changing the bonding temperature. Increasing the $C_{\alpha L}$ value decreases the time required for completion of isothermal solidification and also the time required for homogenisation. Thus, the time required for completion of the entire TLP bonding process (dissolution, isothermal solidification, and homogenisation) will not be affected by an increase in the $C_{\alpha L}$ value.

It has been suggested that selection of the optimum bonding temperature during TLP bonding depends on the interplay of increasing solute diffusivity and decreasing equilibrium solute concentration in the

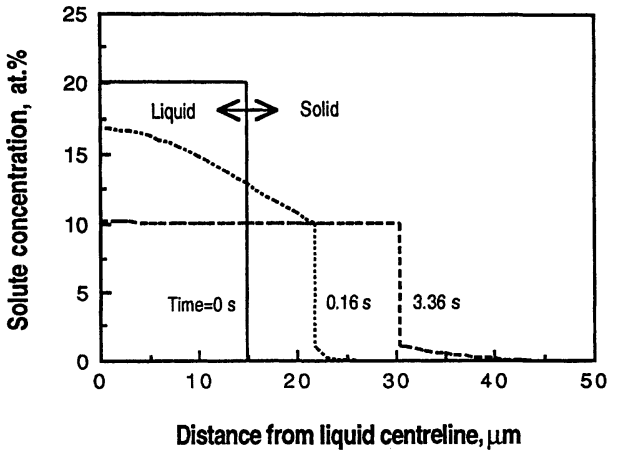


**8 Change in solute concentration profile during base metal dissolution stage (after Ref. 68)**

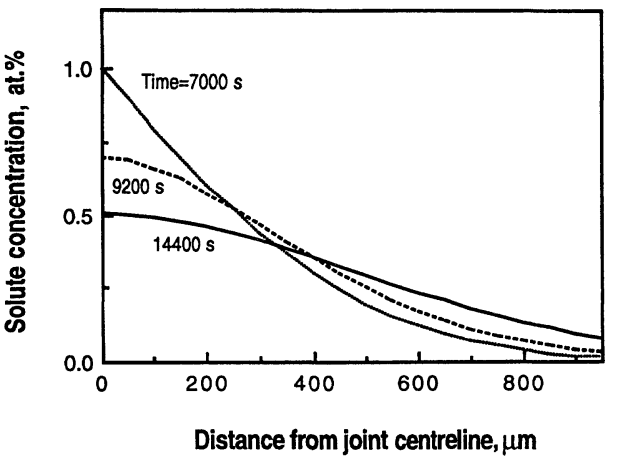


**10 Change in solute concentration profile during homogenisation stage (after Ref. 68)**

solid.[8] However, this idea is based wholly on a consideration of the isothermal solidification stage during TLP bonding; the critical homogenisation stage during TLP bonding is not taken into account. Since variation of the equilibrium solute concentration in the solid has no influence on the time required for completion of the whole TLP bonding operation, the highest possible bonding temperature should be selected during joining. This will increase the rate of solute diffusion into the base metal. In practice, the maximum bonding temperatures will be limited by the need for compatibility with the heat treatment requirements of the base material.[84]

### Comparison of numerical and analytical output

In the analytical approach, it is assumed that movement of the solid/liquid interface $Y$ during isothermal solidification obeys a parabolic law

$$Y = 2\beta(t^{1/2}) = 2K(D_S t)^{1/2} \quad . \; . \; . \; . \; . \; . \; . \; . \quad (25)$$

where the constant $\beta$ defines the rate of interface movement. During numerical calculations, $\beta$ is evaluated using the relation

$$\beta = \frac{1}{2}\frac{\mathrm{d}Y}{\mathrm{d}(t^{1/2})} = (t)^{1/2}\frac{\mathrm{d}Y}{\mathrm{d}t} \quad . \; . \; . \; . \; . \; . \; . \; . \; . \quad (26)$$

The $\beta$ parameter is a particularly useful means of comparing the output of analytical and numerical calculations. Figure 12 shows the variation of the $\beta$ parameter during base metal dissolution and subsequent isothermal solidification for a hypothetical TLP bonding situation.[68] The value of $\beta$ decreases progressively and approaches zero when base metal dissolution is almost completed. In fact, $\beta$ decreases to a value of $-0{\cdot}185\ \mu\mathrm{m\ s}^{-1/2}$ and this is identical to the analytical solution (equation (20)). Thus, the isothermal solidification stage during TLP bonding can be readily estimated using an analytical solution; for example, Fig. 13 shows the results when nickel base material is TLP bonded using Ni–B filler metal.[31] In direct contrast, base metal dissolution depends on a non-parabolic relation, and no single value of $\beta$ can characterise solid/liquid interface movement.

The remarkable difference between the output of numerical and analytical solutions during base metal dissolution and isothermal solidification occurs because the analytical calculations assume that solute diffusion occurs wholly in solid state and that liquid phase is not formed during the joining operation.

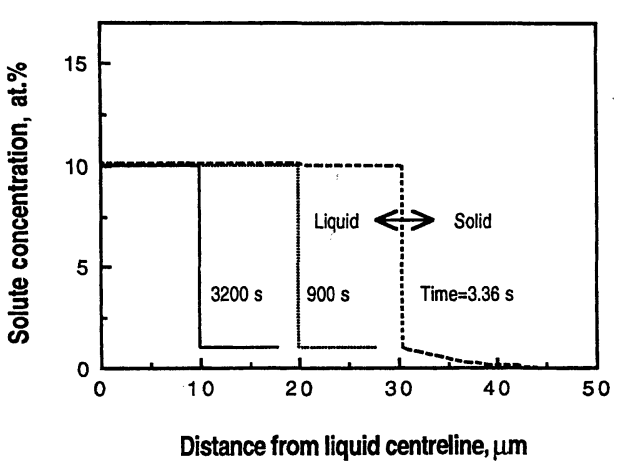


**9 Change in solute concentration profile during isothermal solidification stage (after Ref. 68)**

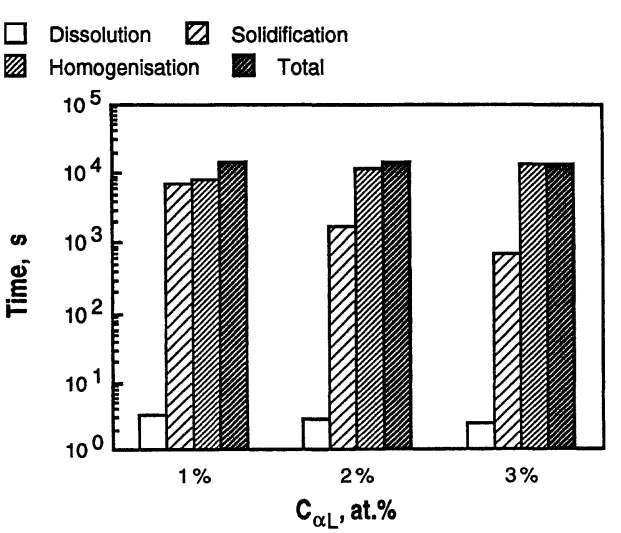


**11 Effect of solidus composition at bonding temperature $C_{\alpha L}$ on completion times required for dissolution, isothermal solidification, and homogenisation (after Ref. 68)**

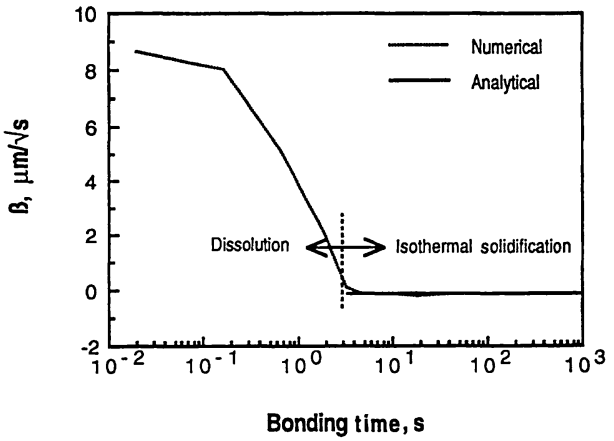


**12 Comparison between numerical and analytical calculated $\beta$ values, where the constant $\beta$ defines the rate of interface movement (after Ref. 67)**

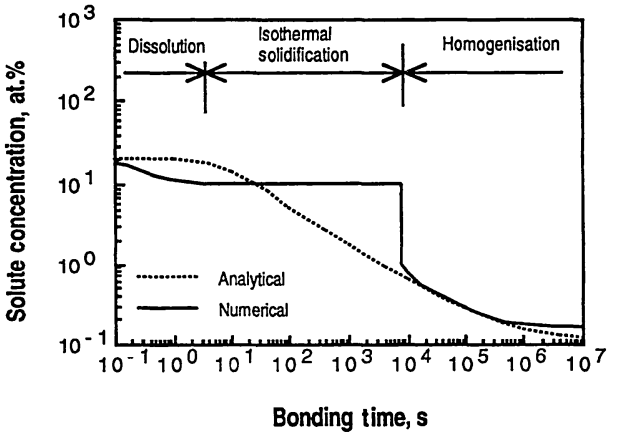


**14 Calculated changes in solute concentration at specimen centreline during TLP bonding (after Ref. 68)**

Figure 14 compares the results of analytical and numerical calculations of the homogenisation stage during TLP bonding. Numerical and analytical results are in close agreement during part of the homogenisation stage, although differences are apparent early and late in the processing cycle. The deviation between the numerical and analytical results late in the homogenisation stage (in Fig. 14) results from the semi-infinite test specimen assumption in the analytical calculations.

It can be concluded, therefore, that simple analytical solutions can be used to estimate the completion times for isothermal solidification and for estimating the solute concentration at the joint centreline. It should be noted that the error function required in the analytical solution must be found by solving equation (20) numerically. Also, direct parameter input into a numerical program can permit ready prediction of the completion times for dissolution, isothermal solidification, or homogenisation (for any chosen bonding temperature and filler metal–base metal combination).

## Modelling of real systems

Much research to date on modelling of TLP bonding has involved two aspects. The first aspect is one-dimensional modelling only. However, when Tuah-Poku *et al.*[8] compared their analytically calculated and experimental completion times for isothermal solidification during TLP bonding of silver using copper filler metal, they observed a marked difference in these results. They suggested that this difference might be due to liquid penetration at grain boundaries in the base metal (this increased the solid/liquid interfacial area for solute diffusion). This effect has been confirmed in research by Kokawa *et al.*[85] and Saida *et al.*[86] (Fig. 15). With this in mind, one dimensional modelling results are really only useful when single crystal or very coarse grained polycrystal substrates are joined using TLP bonding.

The second aspect is the solution of a two phase moving interface problem in a simple binary alloy system, e.g. pure nickel base material bonded using a Ni–P interlayer. The implicit assumptions are that local equilibrium exists at the migrating interface during TLP bonding, and that formation of an intermediate phase does not occur during isothermal solidification. However, this is an approximation since local equilibrium is generally not attained at the solid/liquid interface.[73] Furthermore, direct experimental evidence has been presented by Gale and Wallach[64]

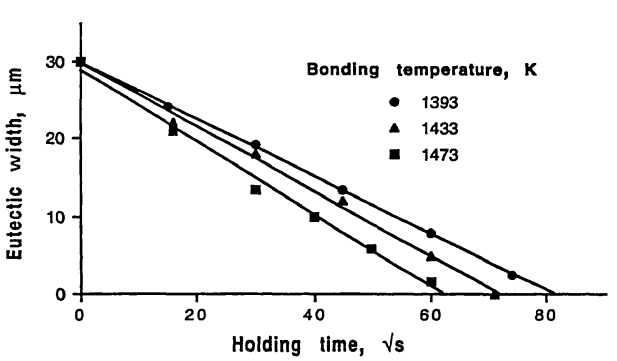


**13 Relation between holding time at different bonding temperatures and eutectic width during TLP bonding of nickel base material using Ni–B filler metal (after Ref. 31)**

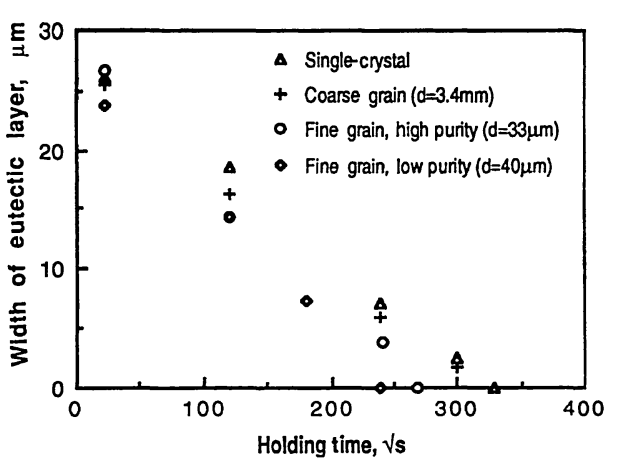


**15 TLP bonding of nickel base metals with different grain sizes; *d* is mean grain size before TLP bonding (after Refs. 85, 86)**

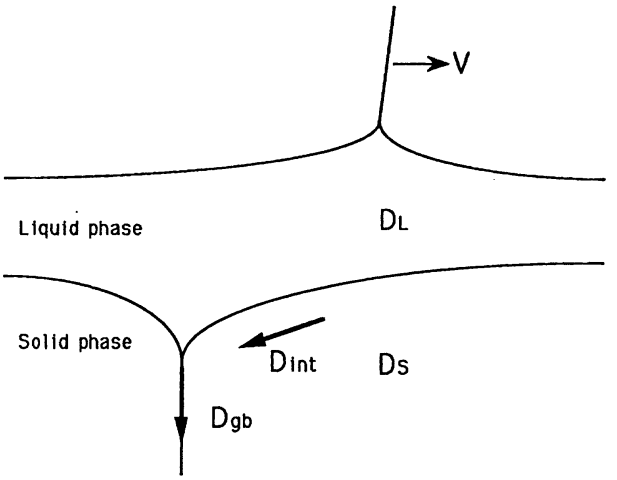


**16 Schematic showing factors in two dimensional model of TLP bonding ($D_L$, $D_S$, $D_{gb}$, and $D_{int}$ are diffusion coefficients in liquid, solid, grain boundary and liquid/solid interface regions, respectively)**

for the formation, at the bonding temperature, of an intermediate phase ($Ni_3B$) during TLP bonding of nickel base material using Ni–Si–B filler metal. In addition, it has been reported that partial or complete homogenisation can occur in some regions of NiAl/Ni–Si–B/NiAl joints while isothermal solidification is still taking place in adjacent regions.[17,18]

## Effect of base metal grain boundaries on process kinetics

Since TLP bonding is a diffusion controlled process, any factor that affects diffusion will alter the process kinetics during the joining operation. When single crystal base material is TLP bonded, solute transport depends on volume diffusion in the solid and in the liquid. However, when a polycrystalline base metal is TLP bonded, solute diffusion will depend on a number of factors (*see* Fig. 16).

1. Grain boundary diffusion: diffusivity is much higher at grain boundary regions than in the bulk material when the temperature $T$ is in the range $T < 0{\cdot}5$–$0{\cdot}75T_m$ (where $T_m$ is the equilibrium melting temperature, K).[87] At such temperatures the $D_{gb}/D_l$ ratio is $10^5$ or higher where $D_{gb}$ and $D_l$ are the diffusion coefficients in the grain boundary region and the lattice, respectively.
2. Interface curvature: liquid/solid interface curvature promotes interfacial diffusion which is faster than in the bulk base material.[88]
3. Changes in the solid/liquid interfacial area: since TLP bonding is essentially a homogenisation process in which solute continuously diffuses from the liquid zone into the base metal solid, increasing the solid/liquid interfacial area (as a result of liquid penetration and grain boundary grooving) will increase the transport area for solute diffusion.[85,86]
4. Grain boundary migration: grain boundary migration (as a result of grain growth during the TLP bonding operation) will mean that the solute has more chance of intersecting with grain boundaries. This will affect the solute diffusion rate and therefore the process kinetics.[89]

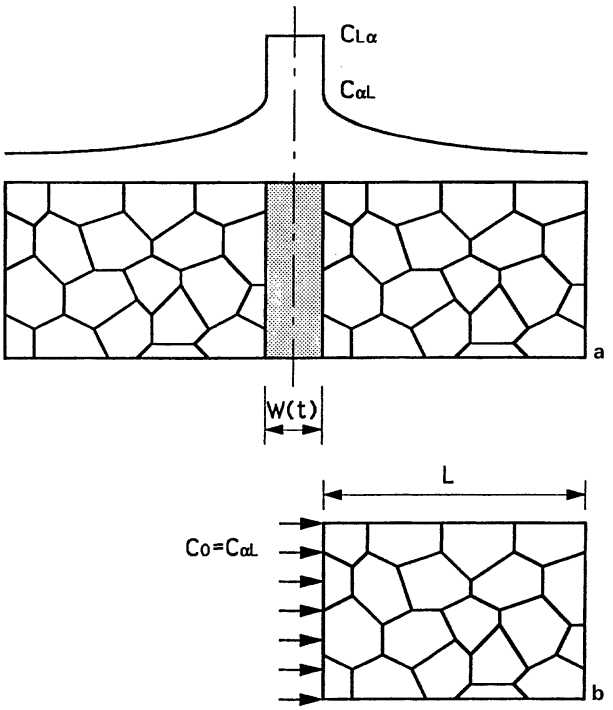


*a* isothermal solidification stage; *b* exchange experiment model

**17 Development of grain boundary model for analysing TLP bonding**

5. Segregation to grain boundaries: factors such as grain boundary segregation will influence the grain boundary free energy and solute diffusivity.[90]

*Grain boundary diffusion model* Diffusion along stationary and moving grain boundaries has been extensively modelled, e.g. by Fisher,[91] Whipple,[92] Suzuoka,[93] Glaeser and Evans,[94] Mishin and Razumovskii,[95] Cermak,[96] and Zhou and North.[97,98] In this connection, only Zhou and North[97,98] have directly examined the effects of base material grain boundaries on solute diffusion and isothermal solidification during TLP bonding.

The rate of isothermal solidification during TLP bonding depends on the amount of solute that diffuses across the interface between the liquid and the base metal[8] and therefore

$$[W_{max} - W(t)]C_{L\alpha} = 2M(t) \quad . \quad . \quad . \quad . \quad . \quad . \quad (27)$$

where $W$ is the liquid width during TLP bonding, $W_{max}$ the maximum liquid width, $C_{L\alpha}$ the solute concentration in liquid at the interface during isothermal solidification, and $M(t)$ the amount of solute that diffuses into the base metal in an exchange experiment (*see* Fig. 17). It follows that the process kinetics during isothermal solidification can be effectively described using $M(t)$, the amunt of solute diffused rather than $W(t)$, the liquid width present during TLP bonding. In other words, calculating the change in the amount of solute diffused with processing time provides a useful indication of the process kinetics during TLP bonding. With this in mind, a numerical model was developed that accounted for the influence of high solute diffusivity at grain boundary regions and of grain boundary migration on the total amount diffused during the isothermal solidification stage of TLP bonding.[97,98]

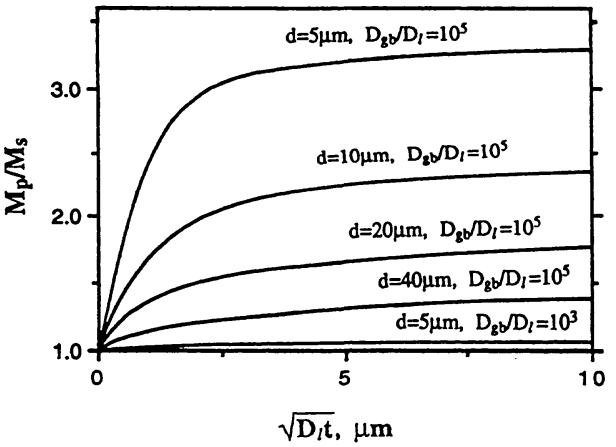


**18 Effect of grain size and of $D_{gb}/D_l$ on $M_p/M_s$ ratio ($D_l$ is lattice diffusion coefficient, $M_p$ is total amount diffused into polycrystalline material, and $M_s$ is total amount diffused in single crystal base metal) (after Ref. 96)**

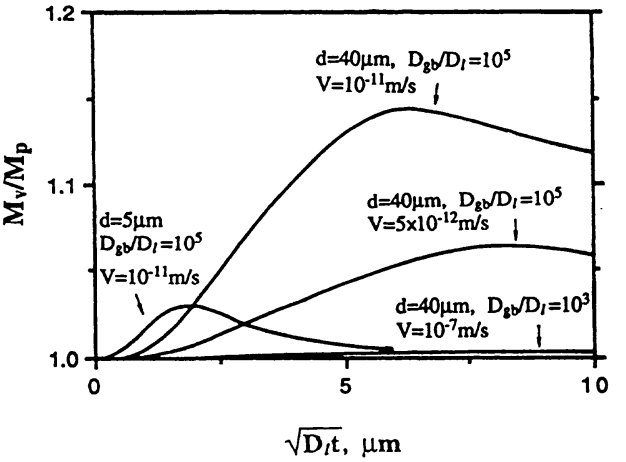


**19 Effect of grain boundary migration on $M_v/M_p$ ratio ($M_v$ is total amount diffused into polycrystalline material containing migrating grain boundaries, $M_p$ is total amount diffused into polycrystalline material when grain boundaries are stationary) (after Ref. 69)**

The influence of grain boundary diffusivity and of grain size on the ratio of $M_p/M_s$ is shown in Fig. 18, where $M_p$ is the total amount diffused into a polycrystalline material and $M_s$ the total amount diffused in a single crystal base metal. It is apparent that the influence of grain boundary regions on solute diffusion depends on the grain size and on the $D_{gb}/D_l$ ratio (where $D_{gb}$ is the grain boundary diffusion coefficient and $D_l$ the lattice diffusion coefficient). The contribution resulting from grain boundary diffusion increases when the grain size becomes smaller. As pointed out earlier, the $D_{gb}/D_l$ ratio is $10^5$ or higher at temperatures in the range $T<0{\cdot}5$–$0{\cdot}75T_m$ (where $T_m$ is the equilibrium melting temperature of the material in kelvin). The influence of grain boundaries on diffusional transport will be much greater under these conditions. However, at high temperatures ($T>0{\cdot}75T_m$), the $D_{gb}/D_l$ ratio is $10^3$ or less, and consequently Fig. 18 indicates that the contribution resulting from grain boundary diffusion will be much less. In this context, the bonding temperature during TLP bonding of nickel base superalloy base material is typically around 1373 K and the $T_b/T_m$ ratio is consequently about 0·8. As a result, there will be a relatively small contribution resulting from grain boundary diffusion when nickel base superalloy material is TLP bonded.

The influence of grain boundary migration on the $M_v/M_p$ ratio is shown in Fig. 19, where $M_v$ is the total amount diffused into a polycrystalline material that contains migrating grain boundaries, and $M_p$ the total amount diffused into a polycrystalline material when the grain boundaries are stationary. Grain boundary migration speeds up mass transfer during part of the holding period, and during this period more diffusion occurs when the grain size, the rate of the grain boundary migration and the $D_{gb}/D_l$ ratio are increased.

*Liquid penetration model* A detailed explanation of the grain boundary grooving phenomenon was first proposed by Mullins.[88,99] The kinetics of grain boundary grooving were analysed when a bicrystal contacted a saturated fluid phase (liquid or gas) at sufficiently high temperature. Grooving occurred as a result of surface diffusion, volume diffusion in the fluid and evaporation/condensation. Gjostein[100] and Robertson[101] confirmed Mullins' theoretical predictions when examining grain boundary grooving in the copper–liquid lead system. Further support was provided by Allen,[102] when examining chromium, molybdenum, and tungsten alloyed with rhenium. Ho and Weatherly[103] applied Mullins' model to a solid–solid system and Robertson[104] extended Mullins' analysis of grain boundary grooving to the case where the groove angle varied. Also, Hardy *et al.*[105] generalised Mullins' theory to the entire range of dihedral angle values through the use of a boundary integral formulation of the free boundary problem. Hackney and Ojard[106] examined grain boundary grooving caused by evaporation or by surface diffusion in a finite system, and Srinivasan and Trived[107] evaluated grooving produced by the concomitant action of surface and volume diffusion. Finally, Vogel and Radke[108] combined volume diffusion in the melt and grain boundary diffusion into one mathematical formulation to explain the formation of deep channel-like grooves at grain boundary intersections with a solid/liquid interface (during isothermal solidification of Al–bicrystal couples in contact with an In–Al melt). Their model is essentially an extension of Mullins's derivation for grain boundary grooving resulting from the combined action of volume and grain boundary diffusion.

As pointed out in the section, 'Effect of base metal grain boundaries on process kinetics', above, the driving force for interface migration emanates from interfacial curvature. Consequently, a flat interface that has no intersection with a grain boundary will not migrate. This is a quite different situation from that during TLP bonding. The driving force for interface migration during TLP bonding results from the concentration gradient in each phase, and interface migration will occur even when the interface

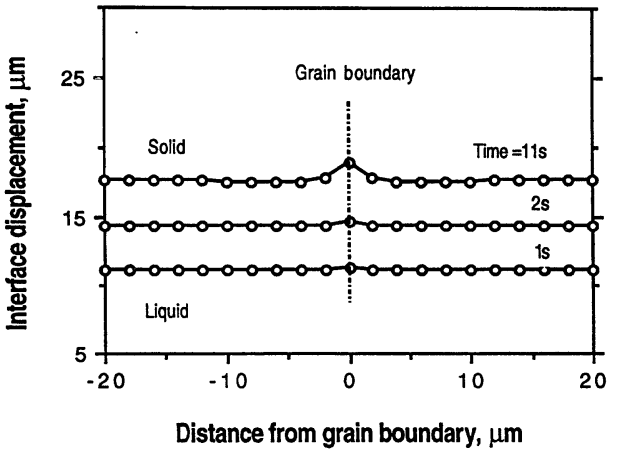


**20 Evolution of profile of liquid/solid interface during dissolution stage (after Ref. 69)**

is flat and there is no grain boundary intersection (e.g. in a single crystal bonding situation). The material transport mechanisms comprise volume diffusion in each phase, interfacial diffusion, and grain boundary diffusion. The classical grain boundary grooving theories proposed by Mullins[88,99] involve extremely complex analytical solutions. As a result, it is difficult to apply Mullins' derivations during TLP bonding, since several diffusion mechanisms operate and finite geometries exist. With this in mind, a numerical model was developed that predicts the extent of interface migration under the combined driving forces of concentration and interfacial curvature gradients.

Ikeuchi *et al.*[69] simulated liquid/solid interface migration at grain boundary regions during TLP bonding of nickel base metal using Ni–19 at.-%P filler metal. Figures 20 and 21 show the evolution of the liquid/solid interface profile at the bonding temperature. Based on Fig. 20, the liquid/solid interface is almost planar during the base metal dissolution stage, and liquid penetration at the grain boundary region is only apparent near the end of the dissolution process. From Fig. 21 it can be seen that liquid penetration is more pronounced when the holding time increases during the isothermal solidification

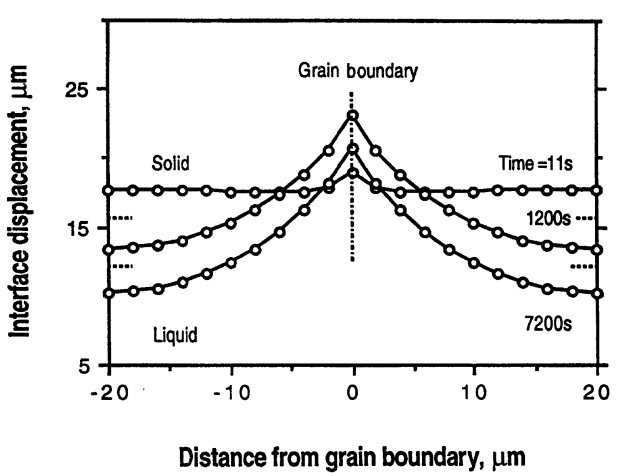


**21 Evolution of profile of liquid/solid interface during isothermal solidification stage (after Ref. 69)**

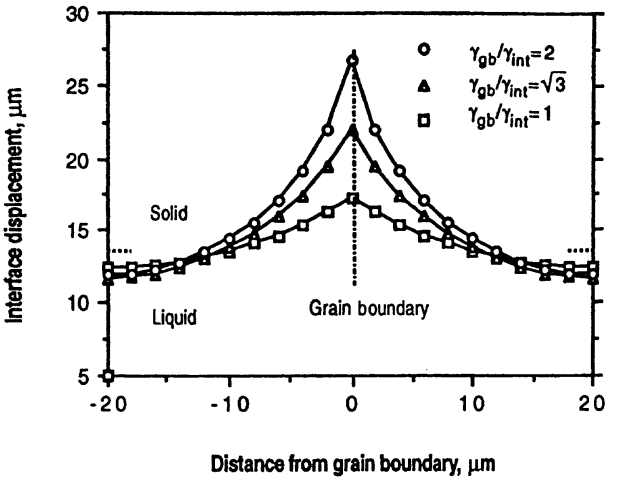


**22 Effect of grain boundary energy on profile of liquid/solid interface during isothermal solidification (after Ref. 69)**

stage. The penetration depth increases to more than 10 μm: large enough to be clearly observed using conventional optical microscopy and scanning electron microscopy. These indications correspond well with the experimental results observed by Saida *et al.*[86] In this connection, Kokawa *et al.*[85] indicated that liquid penetration could not be observed during the dissolution process, but became more pronounced when the holding time increased during the isothermal solidification stage of TLP bonding.

The horizontal broken lines in Fig. 21 indicate the calculated displacement of the liquid/solid interface when the effects of grain boundary related factors are neglected. It is clear that the width of the liquid phase in the bulk region far from the grain boundary (represented by the width at the symmetry axis) is smaller when the influence of grain boundary energy and liquid/solid interfacial energy are taken into account. Thus, the isothermal solidification process in the bulk material is accelerated when the effects of the grain boundary energy and the liquid/solid interfacial energy are taken into account.

The influence of the grain boundary energy on liquid penetration at the grain boundary region is illustrated in Fig. 22. In this figure, the liquid/solid interfacial energy is maintained at 0·424 J $m^{-2}$, and the grain boundary energy is varied from 0·424 to 0·848 J $m^{-2}$. It has already been indicated that the energy of a large angle grain boundary is 0·848 J $m^{-2}$ (Ref. 109). The penetration depth increases, and the angle at which the liquid/solid interface intersects the grain boundary becomes sharper when the grain boundary energy increases. Kokawa *et al.*[85] corroborated these findings during TLP bonding of nickel using Ni–19 at.-%P filler metal.

## Microstructural development in multicomponent systems

Direct experimental evidence for the formation of an intermediate phase at the bonding temperature has been presented by Gale and Wallach.[64] During TLP bonding of nickel base metal using N–Si–B filler metal, $Ni_3B$ formed in substrate material immediately adjacent to the original solid/liquid interface (*see*

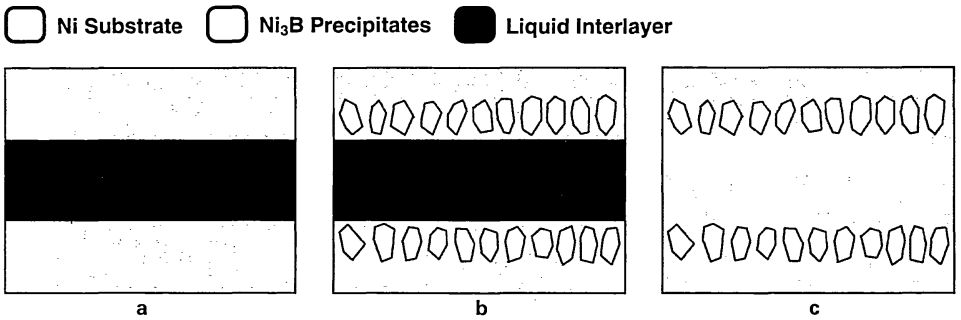


*a* initial as melted geometry; *b* formation of $Ni_3B$ during early stages of bonding; *c* $Ni_3B$ present after completion of isothermal solidification

**23 Schematic showing formation of $Ni_3B$ during isothermal holding of Ni/Ni–Si–B/Ni bonds at temperature below the Ni–B binary eutectic temperature**

Fig. 23). Boride formation only commenced once melting of the interlayer had been completed and was observed in Ni/Ni–Si–B/Ni joints held at temperatures (e.g. 1065°C) below the Ni–B binary eutectic temperature (1093–1095°C (Ref. 110)). In contrast, when bonding temperatures (e.g. 1150°C) in excess of the Ni–B binary eutectic temperature were employed, extensive liquation of the substrates was observed. Once formed, borides precipitated at the bonding temperature remained stable with further change in holding time (Fig. 24). Following completion of isothermal solidification, the borides could be observed as a near continuous band demarcating the original position of the solid/liquid interface.

Gale and Wallach[64] proposed the following mechanism for the formation of borides at the bonding temperature in Ni/Ni–Si–B/Ni joints. They envisaged a situation where local equilibrium was not developed across the solid/liquid interface and, in such circumstances, boron was free to diffuse from the interlayer into the base material immediately after melting of the substrates. Given that interstitial diffusion of boron in nickel is considerably more rapid than substitutional diffusion of silicon, the initially boron free substrates would be converted into a binary Ni–B alloy. Continued boron diffusion would rapidly result in a substrate boron concentration in excess of the boron solubility in nickel (0·3 at.-% at the Ni–B eutectic temperature of 1093–1095°C (Ref. 110)). Subsequent events would depend on the bonding temperature selected. When a bonding temperature greater than the Ni–B binary eutectic temperature is employed, liquation of the substrate would be expected. In contrast, the use of a bonding temperature below the binary Ni–B eutectic temperature would result in the isothermal formation of borides. These predictions correlated with experimental observations of Ni/Ni–Si–B/Ni joints produced both above and below the Ni–B binary eutectic temperature.

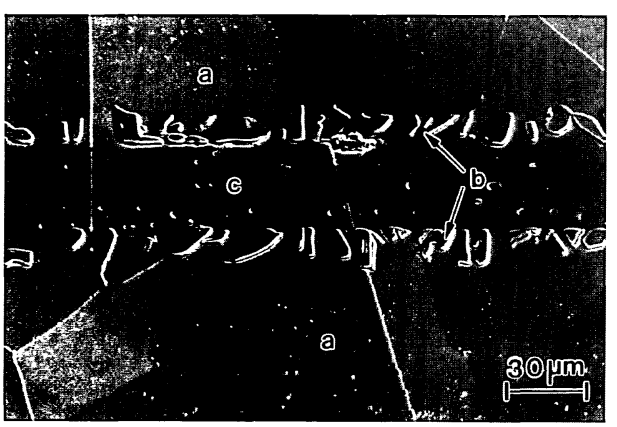


**24 Microstructure of Ni/Ni–Si–B/Ni bond held at temperature of 1065°C for 2 h: $Ni_3B$ precipitates present after completion of isothermal solidification (a Ni substrate; b $Ni_3B$ precipitates; c isothermally resolidified joint) (after Ref. 64)**

In NiAl/Ni–Si–B/Ni joints, Orel *et al.*[17] observed that boride formation and liquation within the nickel substrate proceeded in a manner similar to that in the Ni/Ni–Si–B/Ni system (*see* Figs. 25 and 26). However, in the NiAl substrate, there was no evidence of either the anomalous formation of borides at the bonding temperature or excessive liquation. Instead, boride formation in the NiAl substrate was entirely consistent with precipitation on cooling from the bonding temperature. Orel *et al.*[17] associated these observations with a lower boron diffusivity in NiAl than Ni. Based on the boride precipitation distance from the bondline, the apparent boron diffusivity in NiAl ($\sim 10^{-12}\,m^2\,s^{-1}$) was estimated to be about two orders of magnitude lower than in Ni ($\sim 10^{-10}\,m^2\,s^{-1}$). In such circumstances, anomalous boride formation and liquation dependent upon rapid boron diffusion in advance of the establishment of local solid–liquid equilibrium would only be expected in the Ni substrate and not the NiAl substrate. Hence, microstructural development in the NiAl/Ni–Si–B/Ni system occurs in a manner that is consistent with the processes proposed by Gale and Wallach[64] for Ni/Ni–Si–B/Ni joints.

Le Blanc and Mevrel[36] took boron consumption resulting from boride formation into account when they modelled isothermal solidification during TLP bonding of nickel base superalloy material using a Ni–Si–B filler metal. They found that boron consumption as a result of boride formation accelerated the isothermal solidification process. This particular study employed analytical solutions only, and further work on numerical modelling of this aspect is required.

## Summary

All analytical approaches to the modelling of TLP bonding have treated the joining process as a number of discrete stages; however, this is not what actually

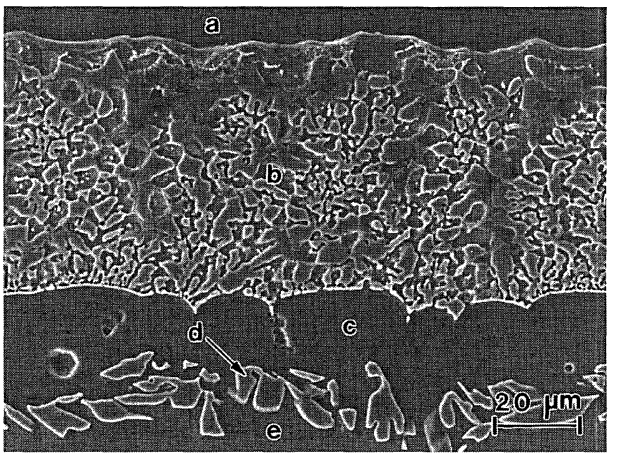


**25 Microstructure of NiAl/Ni–Si–B/Ni bond showing $Ni_3B$ precipitation in Ni substrate: sample held at 1065°C for 5 min (a NiAl substrate; b residual eutectic; c proeutectic Ni; d $Ni_3B$ precipitates; e Ni substrate) (after Ref. 17)**

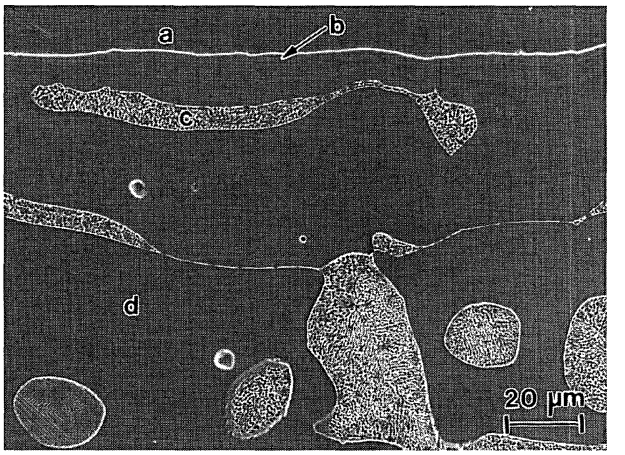


**26 Microstructure of NiAl/Ni–Si–B/Ni bond showing liquation of Ni substrate: sample held at 1150°C for 20 min (a NiAl substrate; b $Ni_3(Al,Si)$; c eutectic deposit in Ni substrate; d substrate Ni phase) (after Ref. 17)**

occurs during the TLP bonding process. Base metal dissolution can not be represented using a parabolic law. However, the isothermal solidification stage can be readily characterised by assuming a linear relation between liquid/solid interface displacement and the square root of the holding time at the bonding temperature. Also, an analytical solution can be used to estimate the solute concentration at the specimen centreline following a given holding period during the homogenisation stage of TLP bonding.

Numerical modelling has the advantage that it can treat base metal dissolution, liquid phase isothermal solidification, and solute homogenisation as sequential steps. It can therefore be readily applied to two- or three-dimensional joining situations when components with complex shapes are fabricated. Liquid/solid interface migration during base metal dissolution, isothermal solidification, and solute redistribution during homogenisation have been simulated using numerical modelling. The optimum joining parameters during TLP bonding have been quantitatively predicted and occur when the solute diffusivity in the liquid and solid phases is increased and when the highest bonding temperature is employed. In addition, the total amount of solute diffused during TLP bonding and grain boundary evolution have been successfully characterised using numerical modelling.

## Future requirements

Future work on the modelling of TLP bonding should involve the development of a general numerical model that encompasses all the transport mechanisms which occur during the TLP bonding process, namely volume diffusion in each phase, grain boundary diffusion, and interfacial diffusion. The driving forces for diffusion consist of the concentration gradients in both the liquid and solid phases, the chemical potential gradients that result from the liquid/solid interfacial curvature gradient, and the grain boundary free energy balance at the grain boundary triple junction. In addition, other factors such as grain boundary segregation will strongly affect the process kinetics during TLP bonding. In this respect, it is worth noting that a general model has already been developed and has been successfully applied during solid state diffusion bonding.[111]

When complex alloys are TLP bonded, much modelling research seems to have proceeded independently of detailed microstructural studies. This has resulted in some of the basic assumptions in modelling not being supported by direct microstructural observations in real joints. In particular, the key assumption that intermediate phase formation does not occur during isothermal solidification is questionable. For example, it has been shown that an intermediate phase ($Ni_3B$) forms at the bonding temperature when Ni and NiAl/Ni base materials are TLP bonded using Ni–Si–B interlayers. With this in mind, there is a critical need for research programmes where modelling output is closely related to detailed microstructural observations. In this connection, phase diagram and diffusivity data are essential requirements for rigorous modelling when multi-element commercial substrates are bonded using filler metals which are available commercially. This type of information is generally unavailable at present and must be developed if modelling and direct experimental observations are to be successfully linked.

## Acknowledgement

The authors would like to thank the Ontario Center for Materials Research for financial support in the prosecution of this research.

## References

1. W. JOST: 'Diffusion in solids, liquids, gases'; 1960, New York, Academic Press.
2. J. CRANK: 'Free and moving boundary problems'; 1984, Oxford, Oxford University Press.
3. R. F. SEKERKA, C. F. JEANFILS, and R. W. HECKEL: in 'Lectures on the theory of phase transformations', (ed. H. I. Aaronson), 117–169; 1975, New York, AIME.

4. A. J. HICKL and R. W. HECKEL: *Metall. Trans.*, 1975, **6A**, 431–440.
5. R. W. HECKEL, A. J. HICKL, R. J. ZAEHRING, and R. A. TANZILLI: *Metall. Trans.*, 1972, **3**, 2565–2569.
6. G. V. KIDSON and G. D. MILLER: *J. Nucl. Mater.*, 1964, **12**, 61–69.
7. W. A. KAYSSER, W. J. HUPPMANN, and G. PETZOW: *Powder Metall.*, 1980, **23**, 86–91.
8. I. TUAH-POKU, M. DOLLAR, and T. B. MASSALSKI: *Metall. Trans.*, 1988, **19A**, 675–686.
9. D. S. DUVALL, W. A. OWCZARSKI, and D. F. PAULONIS: *Weld. J.*, 1974, **53**, 203–214.
10. W. A. OWCZARSKI: *Weld. J.*, 1962, **52**, (2), 78s–83s.
11. E. LUGSCHEIDER, T. SCHITTNY, and E. HALMOY: *Weld. J.*, 1989, **68**, (1), 9s–13s.
12. Y. NAKAO, K. NISHIMOTO, K. SHINOZAKI, and C. Y. KANG: in 'Joining of advanced materials', (ed. T. H. North), 129–144; 1990, London, Chapman and Hall.
13. A. E. DRAY: PhD dissertation, University of Cambridge, 1985.
14. E. R. MADDRELL and E. R. WALLACH: in Proc. Conf. 'Recent trends in welding science and technology', (ed. S. A. David and J. M. Vitek), 1990, Materials Park, OH, ASM International.
15. T. J. MOORE and J. M. KALINOWSKI: in MRS Symp. Proc. on 'High temperature ordered intermetallic alloys V', (ed. I. Baker *et al.*), Vol. 288, 1173–1178; 1993, Pittsburgh, PA, Materials Research Society.
16. M. J. STRUM and G. A. HENSHALL: in Proc. Conf. 'Advanced joining technologies for new materials II', (ed. N. F. Flore and J. O. Stiegler), 76–88; 1994, Miami, FL, American Welding Society.
17. S. V. OREL, L. PAROUS, and W. F. GALE: *Weld. J.*, 1995, **74**, (9), 319s–324s.
18. S. V. OREL, L. PAROUS, and W. F. GALE: in Proc. Conf. 'Advanced joining technologies for new materials II', (ed. N. F. Flore and J. O. Stiegler), 5–9, 1994; Miami, FL, American Welding Society.
19. R. THAMBURAJ, W. WALLACE, and J. A. GOLDAK: *Int. Met. Rev.*, 1983, **28**, (1), 1–22.
20. G. S. HOPPIN and T. F. BERRY: *Weld. J.*, 1970, **49**, (11), 505s–509s.
21. H. IKAWA and Y. NAKAO: *Trans. Jpn Weld. Soc.*, 1977, **8**, 3–8.
22. H. IKAWA, Y. NAKAO, and T. ISAI: *Trans. Jpn Weld. Soc.*, 1979, **10**, (1), 24–29.
23. D. S. DUVALL, W. A. OWCZARSKI, D. F. PAULONIS, and W. H. KING: *Weld. J.*, 1970, **49**, (2), 41s–49s.
24. T. ONZAWA, A. SUZAMURA, and M. W. KO: *J. Jpn Weld. Soc.*, 1989, **7**, (4), 38–45, (in Japanese).
25. W. A. OWCZARSKI: in Proc. Conf. 'Physical metallurgy of metal joining', (ed. R. Kossowsky and M. E. Glicksman); 1980, Warrendale, PA, TMS–AIME.
26. B. JAHNKE and J. DEMNY: *Thin Solid Films*, 1983, **110**, 225–235.
27. T. J. MOORE and T. K. GLASGOW: *Weld. J.*, 1985, **64**, (8), 219s–226s.
28. G. E. SHEWARD: 'High temperature brazing in controlled atmospheres'; 1985, London, Pergamon Press.
29. A. SUZAMURA, T. ONZAWA, and H. TAMURA: *J. Jpn Weld. Soc.*, 1985, **3**, (2), 85–91, (in Japanese).
30. Y. NAKAO, K. NISHIMOTO, K. SHINOZAKI, C. Y. KANG, and Y. HORI: *Q. J. Jpn Weld. Soc.*, 1988, **6**, 519–526.
31. Y. NAKAO, K. NISHIMOTO, K. SHINOZAKI, and C. Y. KANG: *Trans. Jpn Weld. Soc.*, 1989, **20**, 60–65.
32. Y. NAKAO, K. NISHIMOTO, K. SHINOZAKI, and C. Y. KANG: in Proc. Symp. 'Superalloys', (ed. M. Cieslak), 775–783; 1989, Warrendale, PA, TMS.
33. A. RABINKIN: *Weld. J.*, 1989, **68**, (10), 39–45.
34. K. NISHIGUCHI, Y. TAKAKASHI, and A. SEO: *Q. J. Jpn Weld. Soc.*, 1990, **8**, 336–342.
35. M. NAKAHASHI, M. SHIROKANE, and H. TAKEDA: *J. Jpn Weld. Soc.*, 1990, **54**, (7), 826–831, (in Japanese).
36. A. LE BLANC and P. MEVREL: in Proc. Conf. 'High temperature materials for power engineering', (ed. E. Bachelet *et al.*), 1451–1460; 1990, Dordrecht, The Netherlands.
37. T. FUNAMOTO, M. KATO, R. KAJIWARA, K. YASUDA, T. SHIDA, T. MATSUDA, and F. MATSUDA: *Weld. Int.*, 1991, **6**, (4), 270–277.
38. T. FUNAMOTO, M. KATO, R. KAJIWARA, K. YASUDA, T. SHIDA, T. MATSUDA, and F. MATSUDA: *J. Jpn Weld. Soc.*, 1991, **9**, (3), 47–54, (in Japanese).
39. Y. NAKAO, K. NISHIMOTO, K. SHINOZAKI, C. Y. KANG, Y. C. SHIGETA, and H. SHIGETA: *J. Jpn Weld. Soc.*, 1991, **9**, (1), 55–59, (in Japanese).
40. Y. NAKAO and K. SHINOZAKI: *Mater. Sci. Technol.*, 1995, **11**, (3), 304–311.
41. R. R. WELLS and E. B. MIKUS: 'Thin film diffusion brazing of titanium members using copper intermediaries', US Patent 3 417 461, Northrop Hawthorne, CA, 1968.
42. K. C. WU: *Weld. J.*, 1971, **49**, 386s–393s.
43. R. R. WELLS: *Weld. J.*, 1976, **55**, (1), 20s–27s.
44. B. NORRIS: 'Designing with titanium', 83–86; 1986, London, The Institute of Metals.
45. Y. KOMIZO, F. KASHIMOTO, T. TOMITA, and K. OGAWA: *Q. J. Jpn Weld. Soc.*, 1990, **8**, 197–204.
46. T. FUNAMOTO, H. WACHI, R. KAJIWARA, M. KATO, T. MATSUZAKA, and T. SHIDA: *J. Jpn Weld. Soc.*, 1987, **5**, 43–45, (in Japanese).
47. J. T. NIEMANN and R. A. GARRET: *Weld. J.*, 1974, **52**, 175–184.
48. T. ONZAWA, A. SUZAMURA, J. H. KIM, and K. TAKAGAMI: *Weld. Int.*, 1992, **6**, (9), 707–712.
49. T. ONZAWA, A. SUZAMURA, and J. H. KIM: *J. Jpn Weld. Soc.*, 1990, **8**, (4), 74–78.
50. T. ONZAWA, A. SUZAMURA, and J. H. KIM: *J. Jpn Weld. Soc.*, 1990, **8**, (2), 122–128.
51. Z. LI, Y. ZHOU, and T. H. NORTH: *J. Mater. Sci.*, 1995, **11**, April, 363–369.
52. K. KURIYAMA: PhD dissertation, University of Cambridge, 1992.
53. T. MOMONO, S. JACKSON, and E. R. WALLACH: in Proc. Seminar 'Joining of advanced materials', Kobe, Japan, July 1993, Technical Commission on Welding Metallurgy and Interface Joining/JWES Research Commission on Welding of Special Materials, 68–73.
54. Z. LI, W. FEARIS, and T. H. NORTH: *Mater. Sci. Technol.*, 1995, **11**, (4), 363–369.
55. T. FUNAMOTO, H. WACHI, R. KAJIWARA, M. KATO, T. MATSUZAKA, and T. SHIDA: *J. Jpn Weld. Soc.*, 1988, **6**, (2), 23–29, (in Japanese).
56. L. BERNSTEIN: *J. Electrochem. Soc.*, 1966, **113**, 1282–1288.
57. L. BERNSTEIN and H. BARTHOLOMEW: *Trans. AIME*, 1966, **236**, 405–412.
58. R. E. LOEHMANN: in 'Surfaces and interfaces in ceramic and ceramic–metal systems', (ed. J. Pask and A. Evans), 701–711, 1980, New York, Plenum Press.
59. W. FEDUSKA: *Weld. J.*, 1958, **37**, (2), 62s–73s.
60. K. P. GROSSKURTH: *Prakt. Metallogr.*, 1974, **11**, 249–258.
61. R. JOHNSON: *Weld. J.*, 1981, **60**, 10, 185s–193s.
62. B. GRUSHKO and B. Z. WEISS: *Metall. Trans.*, 1984, **15A**, (4), 609–620.
63. A. J. MARKHAM: PhD dissertation, University of Cambridge, 1988.
64. W. F. GALE and E. R. WALLACH: *Metall. Trans.*, 1991, **22A**, 2451–2457.
65. W. D. MacDONALD and T. W. EAGAR: *Annu. Rev. Mater. Sci.*, 1992, **22**, 23–46.
66. H. NAKAGAWA, C. H. LEE, and T. H. NORTH: *Metall. Trans.*, 1991, **22A**, 543–555.
67. Y. ZHOU: PhD dissertation, University of Toronto, 1994.
68. Y. ZHOU and T. H. NORTH: *Z. Metallkd.*, 1994, **85**, 775–780.
69. K. IKEUCHI, Y. ZHOU, H. KOKAWA, and T. H. NORTH: *Metall. Trans.*, 1993, **23A**, (10), 2905–2915.
70. G. LESOULT: 1976, cited in Ref. 8.
71. R. F. SEKERKA: in Proc. Conf. 'Physical metallurgy of metals joining', (ed. R. Kossowsky and M. E. Glicksman), 1–3; 1980, St Louis, MO, TMS–AIME.
72. T. H. NORTH, K. IKEUCHI, Y. ZHOU, and H. KOKAWA: in Proc. Symp. 'The science of metal joining', (ed. M. J. Cieslak *et al.*), 83–91; 1991, Warrendale, PA, TMS.
73. J. S. LANGER and R. F. SEKERKA: *Acta Metall.*, 1975, **23**, 1225–1237.
74. J. CRANK: 'The mathematics of diffusion', 2nd edn; 1975, New York, Oxford University Press.
75. P. G. SHEWMON: 'Diffusion in solids', 2nd edn, 37–39; 1989, Warrendale, PA, TMS.
76. S. LIU, D. L. OLSON, G. P. MARTIN, and G. R. EDWARDS: *Weld. J.*, 1991, **70**, 207s–215s.
77. J. F. LYNCH, L. FEINSTEIN, L. HUGGINS, and R. A. HUGGINS: *Weld. J.*, 1959, **37**, 85s–89s.
78. P. V. DANCKWERTS: *Trans. Faraday Soc.*, 1950, **46**, 701–712.
79. A. SAKAMOTO, C. FUJIWARA, T. HATTORI, and S. SAKAI: *Weld. J.*, 1989, **68**, 63–71.
80. J. E. RAMIREZ and S. LIU: *Weld. J.*, 1992, **71**, 365s–375s.

81. Y. ZHOU and T. H. NORTH: *Model. Simul. Mater. Sci. Eng.*, 1993, **1**, 505–516.
82. R. A. TANZILLI and R. W. HECKEL: *Trans. AIME*, 1968, **242**, 2313–2321.
83. R. A. TANZILLI and R. W. HECKEL: *Metall. Trans.*, 1971, **2**, 1779–1784.
84. E. LUGSCHEIDER, U.-D. PARTZ, and R. LISON: *Weld. J.*, 1982, **61**, 329s–333s.
85. H. KOKAWA, C. H. LEE, and T. H. NORTH: *Metall. Trans.*, 1991, **22A**, 1627–1631.
86. K. SAIDA, Y. ZHOU, and T. H. NORTH: *J. Jpn Inst. Met.*, 1994, **58**, 810–818.
87. N. L. PETERSON: *Int. Met. Rev.*, 1983, **28**, 65–91.
88. W. W. MULLINS: *J. Appl. Phys.*, 1957, **28**, 333–339.
89. G. R. PURDY and Y. J. M. BRECHET: in 'Diffusion analysis and applications', (ed. A. D. Romig, Jr and M. A. Dayananda), 161–189; 1988, Warrendale, PA, TMS.
90. K. AUST and B. CHALMERS: *Metall. Trans.*, 1970, **1**, 1095–1104.
91. J. C. FISHER: *J. Appl. Phys.*, 1951, **22**, 74–77.
92. R. T. P. WHIPPLE: *Philos. Mag.*, 1954, **45**, 1225–1236.
93. T. SUZUOKA: *Trans. Jpn Inst. Met.*, 1961, **2**, 25–33.
94. A. M. GLAESER and J. W. EVANS: *Acta Metall.*, 1986, **8**, 1545–1552.
95. Y. MISHIN and I. M. RAZUMOVSKII: *Acta Metall.*, 1992, **40**, 839–845.
96. J. CERMAK: *Phys. Status Solidi (a)*, 1990, **120**, 351–361.
97. Y. ZHOU and T. H. NORTH: *Acta Metall. Mater.*, 1994, **42**, (3), 1025–1029.
98. Y. ZHOU and T. H. NORTH: in Proc. Seminar 'Joining of advanced materials', Kobe, Japan, July 1993, JWS Technical Commission on Welding Metallurgy and Interface Joining/JWES Research Commission on Welding of Special Materials, 108–117.
99. W. W. MULLINS: *Trans. AIME*, 1960, **218**, 354–361.
100. N. A. GJOSTEIN: *Trans. AIME*, 1961, **221**, 1039–1046.
101. W. M. ROBERTSON: *Trans. AIME*, 1965, **233**, 1232–1236.
102. B. C. ALLEN: *Trans. AIME*, 1966, **236**, 915–924.
103. E. HO and G. C. WEATHERLY: *Acta Metall.*, 1975, **23**, 1451–1460.
104. W. M. ROBERTSON: *J. Appl. Phys.*, 1971, **42**, 463.
105. S. C. HARDY, G. B. McFADDEN, and S. R. CORIELL: *J. Cryst. Growth*, 1991, (114), 467–480.
106. S. C. HACKNEY and G. C. OJARD: *Scr. Metall.*, 1988, **22**, 1731–1735.
107. S. R. SRINIVASAN and R. TRIVED: *Acta Metall.*, 1973, **21**, 611–620.
108. H. J. VOGEL and L. RADKE: *Acta Metall.*, 1991, **39**, 641–649.
109. L. E. MURR: 'Interfacial phenomena in metals and alloys'; 1975, Reading, MA, Addison-Wesley.
110. T. B. MASSALSKI: 'Binary alloy phase diagrams'; 1986, Metals Park, OH, ASM International.
111. A. HILL and E. R. WALLACH: *Acta Metall.*, 1989, **37**, 2425–2437.